## MHC genotyping from rhesus macaque exome sequences

- John R. Caskey<sup>1</sup>, Roger W. Wiseman<sup>1,2</sup>, Julie A. Karl<sup>2</sup>, David A. Baker<sup>1</sup>, Taylor Lee<sup>1</sup>, Muthuswamy
- 4 Raveendran<sup>3</sup>, R. Alan Harris<sup>3</sup>, Jianhong Hu<sup>3</sup>, Donna M. Muzny<sup>3</sup>, Jeffrey Rogers<sup>3</sup>, David H. O'Connor<sup>1,2</sup>
- <sup>1</sup>Wisconsin National Primate Research Center, University of Wisconsin-Madison, Madison, WI 53715,
- 6 USA

11

12

1

2

- <sup>2</sup>Department of Pathology and Laboratory Medicine, University of Wisconsin-Madison, Madison, WI
- 8 53705, USA
- <sup>3</sup>Human Genome Sequencing Center, Baylor College of Medicine, Houston, TX 77030, USA
- 10 Corresponding author: Dr. David H. O'Connor (doconnor@primate.wisc.edu; +1 608 890 0845)

Author	ORCID
Caskey	0000-0001-5665-524X
Wiseman	0000-0002-7682-7085
Karl	0000-0002-4447-4721
Baker	0000-0002-6811-8238
Lee	0000-0002-8768-4358
Raveendran	0000-0001-6185-4059
Jianghong	0000-0002-6318-8595
Harris	0000-0002-7333-4752
Rogers	0000-0002-7374-6490
O'Connor	0000-0003-2139-470X

Keywords: Macaca mulatta, exome, major histocompatibility complex

#### **Abstract**

13

14

15

16

17

18

19

20

21

22

23

24

25

26

27

28

29

Indian rhesus macaque major histocompatibility complex (MHC) variation can influence the outcomes of transplantation and infectious disease studies. Frequently, rhesus macaques are MHC genotyped to identify variants that could account for unexpected results. Since the MHC is only one region in the genome where variation could impact experimental outcomes, strategies for simultaneously profiling variation in the macaque MHC and the remainder of the protein coding genome would be useful. Here we introduce macaque exome sequence (MES) genotyping, in which MHC class I and class II genotypes are determined with high confidence using targetenrichment probes that are enriched for MHC sequences. For a cohort of 27 Indian rhesus macaques, we describe two methods for obtaining MHC genotypes from MES data and demonstrate that the MHC class I and class II genotyping results obtained with these methods are 98.1% and 98.7% concordant, respectively, with expected MHC genotypes. In contrast, conventional MHC genotyping results obtained by deep sequencing of short multiplex PCR amplicons were only 92.6% concordant with expectations for this cohort.

#### Introduction

30

31

32

33

34

35

36

37

38

39

40

41

42

43

44

45

46

47

48

49

50

51

52

53

54

The major histocompatibility complex (MHC) is an intensively studied set of genes in macaques (Shiina et al. 2017; Wiseman et al. 2013). The genomic MHC region contains clusters of genes that encode the MHC class I complex and the MHC class II complex. Cells use MHC class I molecules to present intracellular peptides to immune cells like the CD8+ T cell or natural killer cells (Garcia and Adams 2005). MHC class I molecules accommodate intracellular peptides of varying specificity by having diverse amino acid sequences in the  $\alpha$ 1 and  $\alpha$ 2 subunits, which form the peptide-binding cleft (Silver and Watkins 2017; Loffredo et al. 2009). These  $\alpha$  1 and  $\alpha$  2 subunits correspond to exons 2 and 3, respectively, of an MHC class I gene (Malissen et al. 1982). Most of the polymorphisms that distinguish MHC class I alleles are concentrated in exons 2 and 3 (Williams 2001). Thousands of individual MHC allelic variants have been identified in the three most widely used macaque species for biomedical research: rhesus (Macaca mulatta), cynomolgus (Macaca fascicularis), and pig-tailed macaques (Macaca nemestrina) (Semler et al. 2018; Karl et al. 2017; Maccari et al. 2017). In humans, the MHC is also termed the human leukocyte antigen complex (HLA). HLA class I has a single copy of the HLA-A, HLA-B, and HLA-C genes on each chromosome (Daza-Vamenta et al. 2004; Shiina et al. 2017). In contrast, macaques have a variable number of genes on each chromosome that encode MHC class I MHC-A and MHC-B proteins, and macaques lack an *HLA-C* orthologue (Daza-Vamenta et al. 2004; Shiina et al. 2017; Wiseman et al. 2013). Initial approaches to genotype macaque MHC class I relied on using sequence-specific PCR oligonucleotides to test for the presence or absence of individual alleles (Kaizu et al. 2007). More recently, deep sequencing genomic DNA or complementary DNA PCR amplicons spanning a highly variable region of exon 2 has become commonplace (Wiseman et al. 2009; Karl et al. 2013). Amplicon sequences can be used to genotype groups of closely related MHC class I alleles, which are denoted as lineages. For example, an amplicon deep sequence that corresponds to the rhesus macaque Manu-A1\*001 lineage demonstrates that an animal possesses Manu-A1\*001:01, Mamu-A1\*001:02, or another closely related variant that has not yet been identified. This lineage-level reporting of MHC class I genotypes can be sufficient for designing experiments where certain MHC class I genotypes need to be matched between animals, balanced among experimental groups, or excluded entirely from a study (Loffredo et al.

56

57

58

59

60

61

62

63

64

65

66

67

68

69

70

71

72

73

74

75

76

77

78

79

80

81

2007; Loffredo et al. 2009; Muhl et al. 2002; Karl et al. 2013; Wiseman et al. 2009; Nomura et al. 2012; Mothe et al. 2003). Amplicon deep sequencing can also be used for MHC class II genotyping. The human HLA class II genes DOA1, DOB1, DPA1, and DPB1 have direct orthologues in macaques (Otting et al. 2017). Both macaques and humans have a variable number of MHC class II DRB genes on a single chromosome, while the DRA gene is oligomorphic (Daza-Vamenta et al. 2004; Shiina et al. 2017), and typically is not used for genotyping purposes. MHC class II molecules are members of the immunoglobulin superfamily, but they differ from MHC class I in several ways. The MHC class II complex is comprised of an  $\alpha$  and  $\beta$  subunit heterodimer, and separate genes encode each MHC class II  $\alpha$  and  $\beta$  subunit (Brown et al. 1993). Highly polymorphic regions that are diagnostic for MHC class II allele lineages can be PCR amplified in a manner that is similar to the MHC class I genotyping. The most extensive polymorphism among alleles of the MHC class II genes is found in exon 2 (Williams 2001). Each of the DRB, DOA1, DOB1, DPA1 and DPB1 polymorphic MHC class II genes are sufficiently divergent that separate PCR amplicons are required for deep sequencing (Karl et al. 2014). Comprehensive MHC class I and class II genotyping of macaques by amplicon deep sequencing requires preparation of six separate PCR amplicons for MHC class I and class II DRB, DQA1, DQB1, DPA1, and DPB1 (Karl et al. 2014; Karl et al. 2017). Despite this complexity, a major advantage to amplicon deep sequencing has been its cost effectiveness. The output from a single MiSeq sequencing run can be used to determine the MHC class I and MHC class II genotypes for up to 192 macaque samples. In recent years, improved sequencing hardware and software have prompted new approaches to MHC genotyping. Instead of a utilizing PCR amplicons of variable gene regions to genotype samples, researchers can use human whole exome sequencing (WES) and whole genome sequencing (WGS) datasets to determine HLA genotypes (Xie et al. 2017; Kishikawa et al. 2019; Yang et al. 2014; Posey et al. 2016). Likewise, target capture approaches have been described for HLA genotyping with next-generation sequencing (Cao et al. 2013; Wittig et al. 2015). In contrast, MHC genotyping of macaques from WGS (Xue et al. 2016; Bimber et al. 2017; de Manuel et al. 2018) or whole exome sequence (Vallender 2011; Cornish et al. 2016) datasets have not been reported to date. This reflects the challenges presented by mapping short sequence reads against complex, duplicated gene families like the MHC class I genes of macaques where genomic reference

sequences and reference databases of known alleles are incomplete (Zimin et al. 2014; Maccari et al. 2017). In an

era where the per-base cost of sequencing is dropping rapidly, we explored the feasibility of obtaining whole exome sequencing data while maintaining parity of results with the traditional MHC PCR amplicon approach.

Here we introduce MHC genotyping via macaque exome sequencing (MES), which is an exome sequencing-based workflow for comprehensive MHC class I and class II genotyping in macaques. This workflow uses a commercially available human exome target-capture enrichment kit in conjunction with specialized spike-in target-capture probes to specifically cope with the high copy number of macaque MHC genes. We show that accuracy of Indian rhesus macaque MHC class I and class II results from this workflow are comparable to conventional MiSeq genotyping when using exon 2 reference sequences.

#### **Methods**

91

92

93

94

95

96

97

98

99

100

101

102

103

104

105

106

107

108

109

110

111

112

113

114

**Animals** Twenty-seven whole blood samples were collected from Indian rhesus macagues (Macaca mulatta). Five of these samples came from a breeding group of animals living at the Wisconsin National Primate Research Center (WNPRC). The remaining 22 samples were provided by Dr. Michele Di Mascio from the National Institutes of Health's National Institutes of Allergy and Infectious Diseases. Blood sampling was performed under anesthesia and in accordance with the regulations and guidelines outlined in the Animal Welfare Act, the Guide for the Care and Use of Laboratory Animals, and the Weatherall report (Animal Welfare Act 1966; Weatherall 2006). Data Exome sequence datasets have been deposited in the sequence read archive (SRA) under BioProjects PRJNA529708 and PRJNA527214. Fasta reference sequences used for MHC genotyping, and sequence analysis scripts are available from https://go.wisc.edu/jb0926. MHC class I and class II genotyping by amplicon deep sequencing Genomic DNA was isolated from 250µL of whole blood using a Maxwell® 48 LEV Blood DNA Kit (Promega Corporation, Fitchburg, WI). Following isolation, DNA concentrations were determined with a Nanodrop 2000 and samples were normalized to 60 ng/ul. MHC class I and class II PCR amplicons were generated using exon 2-specific primers with adapters (CS1 and CS2) necessary for 4-primer amplicon tagging with the Fluidigm Access Array™ System (Fluidigm, San Francisco, CA, USA) by previously described methods (Karl et al. 2017; Karl et al. 2014). Pooled PCR products were purified using the AMPure XP beads (Agencourt Bioscience Corporation, Beverly, MA, USA) and quantified using the Quant-iT dsDNA HS Assay kit with a Qubit fluorometer (Invitrogen, Carlsbad, CA, USA), following the manufacturer's protocols. The MHC exon 2 genotyping amplicon pools were sequenced on an Illumina MiSeq instrument (San Diego, CA, USA) as previously described (Karl et al. 2017). Analysis of the MiSeq exon 2 genotyping amplicon sequences was performed using a custom Python workflow. The workflow contained a step to remove oligonucleotide primers and sequencing adapters with bbduk, merge a step to

reads bbmerge, a step to identify unique sequences/remove chimeras with USEARCH, and finally mapping unique reads against a deduplicated reference database of rhesus macaque partial MHC class I and class II exon 2 sequences with bbmap (Bushnell et al. 2017; Edgar 2010). The database was derived from sequences in the IPD-MHC NHP database downloaded from the European Bioinformatics Institute website (Maccari et al. 2017). For this publication, we define "IPD exon 2" as this database of reference sequences. SAM output files from bbmap were parsed with the Python package pandas to enumerate the reads from each animal that were identical to IPD exon 2 reference sequences. *Mamu-A*, -B, -DRB, -DQA1, -DQB1, -DPA1 and -DPB1 lineage-level haplotypes were inferred for each of the samples with a semi-automated custom workflow that identifies diagnostic alleles associated with previously defined rhesus macaque haplotypes (Karl et al. 2013; Otting et al. 2017).

#### MHC class I and class II genotyping by exome sequencing

115

116

117

118

119

120

121

122

123

124

125

126

127

128

129

130

131

132

133

134

135

136

137

138

139

140

141

Genomic DNA was isolated as described above and shipped to the Human Genome Sequencing Center at the Baylor College of Medicine. MHC and exon-containing genomic DNA fragments were selectively enriched using a custom target-capture probeset. Genome-wide exons were captured using SegCap EZ HGSC VCRome2.1, an optimized human clinical exome probeset (Clark et al. 2013, Yang et al. 2013). SeqCap EZ HGSC VCRome2.1 contains probes designed to enrich 23,585 human genes and 189,028 non-overlapping exons. A low coverage audit was performed to identify rhesus macaque exons inferred from the reference genome rheMac2 that were not sufficiently enriched (<20x coverage) with these human probes, and an additional 22,884 rhesus macaque exons were incorporated into the genotyping probe design (Prall et al. 2017). Finally, and most importantly for MHC analyses, we modified the SeqCap EZ Design: Human MHC Design to selectively enrich MHC class I and class II sequences. This previous design was prepared by the Beijing Genome Institute in collaboration with Roche/Nimblegen and it targeted the complete 4.97Mb HLA region with non-redundant probes designed against 8 fully sequenced HLA haplotypes (Horton et al. 2008; Cao et al. 2013). For our macaque studies, we prepared a minimal MHC target capture design using a subset of these probes that are based on all functional HLA class I (HLA-A, -B, -C, and -E) and class II (HLA-DRA, -DRB1, -DRB3, -DRB4, -DRB5, -DQA1, -DQB1, -DPA1 and -DPB1) genes. Probes were included to capture complete gene sequences (exons + introns + 3' UTR) as well as ~1 kb of 5' upstream flanking sequence. The BED file of rhesus rheMac2 target coordinates lifted over to rheMac8 was used to prepare this combined minimal MHC and supplemental rhesus spike-in probe design. Because derivation of MHC results from

143

144

145

146

147

148

149

150

151

152

153

154

155

156

157

158

159

160

161

162

163

164

165

166

167

genotyping is paramount, we used a ratio of 2.5x spike-in probes to 1x VCRom2.1 probes. The supplemental probes for MHC and rhesus macaque were a single reagent, and the MHC-specific probes only constituted 609 kb of the 37.9 Mb probes (Prall et al. 2017). An Illumina paired-end pre-capture library was constructed with 750 nanograms of DNA, as described by the Baylor College of Medicine Human Genome Sequencing Center. Pre-capture libraries were pooled into 10-plex library pools for target capture according to the manufacturer's protocol. Samples were pooled in 10-plex sequence capture library pools for 151 bp paired-end sequencing in a single lane of an S4 flow cell on an Illumina Novaseq 6000 at the Baylor College of Medicine Human Genome Sequencing Center. Enumeration of MHC reads in exome data The effective enrichment of MHC reads in the exome datasets was calculated by mapping the reads of each sample's exome dataset against an individual genomic reference file for each individual locus: HLA-A exons 2-3 (NCBI Gene ID: 3105) and HLA-E exons 2-3 (Gene ID: 3133); HLA-DPA1 exons 2-4 (Gene ID: 3113); HLA-DPB1 exons 2-4 (Gene ID: 3115); *HLA-DQA1* exons 2-4 (Gene ID: 3117); *HLA-DQB1* exons 2-4 (Gene ID: 3119); *HLA-DRB1* exons 2-4 (Gene ID: 3123), HLA-DRB3 exons 2-4 (Gene ID: 3125), HLA-DRB4 exons 2-4 (Gene ID: 3126) and HLA-DRB5 exons 2-4 (Gene ID: 3127). This mapping was done by using bbmap with default parameters, which corresponds to a minimum alignment identity of approximately 76% (Bushnell et al. 2017). Empirically, these mapping parameters are sufficient to map macaque MHC reads to their human orthologues. Mapped reads were written to a new fastq file using bbmap's outm= parameter. To quantify the total number of reads in a sample and the number of reads extracted with our reference file, we created a custom Python script, which is available to download. MHC genotyping from exome data Two complementary data analysis strategies were employed to analyze the exome sequence data, and to verify reproducibility and confidence in the MHC genotyping results. For accuracy and quantification purposes, the expected MHC genotypes for each animal were established based on concordance among at least two out of the three described strategies and biological plausibility, e.g., no more than two alleles per Mamu-DQA1, -DQB1, -DPA1, or-DPB1 locus.

Strategy 1: MHC genotyping using Diagnostic Sub-Region (DSR)

168

169

170

171

172

173

174

175

176

177

178

179

180

181

182

183

184

185

186

187

188

189

190

191

The Diagnostic Sub-Region (DSR) was an intra-allelic region that encompassed polymorphisms, and these polymorphisms were distinguishable from alleles with similar sequences. Therefore, this method ensured the DSR was captured in at least one read for each called allele. MHC class I and class II reads initially were extracted from each animal by mapping the FASTQ reads to HLA class I and class II reference sequences containing exons 2-3 and exons 2-4, respectively, plus the intervening intron(s) as described above in 'Enumeration of MHC reads in exome data'. Reads were mapped to these reference sequences using bbmap with default parameters and the parameter (qtrim=lr) (Bushnell et al. 2017). Following extraction of MHC reads from the total exome sequences, the MHC reads were prepared for assembly using a modified version of a data pre-processing pipeline, which included tools from the BBTools package (Bushnell et al. 2017). Briefly, optical duplicates and reads from low-quality regions of the sequencing run were removed. Next, Illumina sequencing adapters were trimmed from the ends of sequencing reads. Any residual spikein or PhiX sequences that inadvertently survived mapping to HLA class I and class II were then removed. Three rounds of error-correction and read merging were performed to create high-confidence merged reads that were wellsupported by common kmers found in the extracted MHC reads. The error-corrected reads were not merged with a minimum overlap, but instead were separately mapped against the IPD exon 2 sequences using bbmapskimmer. The default settings for the software tool bbmapskimmer were used with the following modified parameters (semiperfectmode=t ambiguous=all ssa=t maxsites=50000 maxsites2=50000 expectedsites=50000) (Bushnell et al. 2017). The semiperfectmode setting accepted reads with perfect matches, as well as reads that extended off the end of contigs for no more than half of the length of the mapped read segment. The ambiguous setting and the 'expectedsites' setting reported the first 50,000 matched read segments that met the 'semiperfectmode' filtering, which was set exceedingly high in order to exhaustively map our IPD exon 2 reference file of ~1600 alleles. Using semiperfect mode, these were the segment sequences with the longest matching length. This output file included all mapped reads to all IPD exon 2 reference allele sequences.

We then used samtools mpileup with the settings (-A -a --ff UNMAP -x -B -q 0 -Q 0) on the bbmapskimmer output to calculate a depth of coverage at each position for each IPD exon 2 sequence. Next, we removed any aligned reads to the IPD exon 2 database sequences that contained less than a minimum depth of coverage of two across the entire reference sequence. For ambiguously-mapped reads, the alignments with the longest-matching region were selected for further analysis; ties among alignments were counted multiple times. To reduce the number of false positives, we used Python pandas to only report database sequence matches that had at least one unambiguously mapped read. Based on these mapping parameters, unambiguously-mapped reads must span the DSR. The MHC genotypes from this method were reported as the minimum depth of coverage for each IPD exon 2 database sequence per animal.

Strategy 2: De novo reconstruction of MHC sequences from exome reads

Most *de novo* sequence assemblers have been optimized for resolving long contigs, and are tolerant of small sequence mismatches that can otherwise fragment assemblies. In the case of MHC alleles, however, such closely related sequences were often biologically distinct. Because of the gene duplications in the macaque MHC, there were many valid MHC contigs that could be assembled from a single sample within the exome data. This is conceptually similar to the computational challenge of assembling viral haplotypes, where rapidly evolving viruses such as human immunodeficiency virus accumulate variants that frequently co-segregate as minor populations within an infected person (Baaijens et al. 2017). Therefore, we utilized the overlap assembly algorithm SAVAGE, originally designed to reconstruct viral haplotypes, to reconstruct MHC allele sequences from exome reads (Baaijens et al. 2017). Similar to Strategy 1 above, HLA-mapped reads were pre-processed using the BBTools package to remove low quality reads and optical duplicates. Next, adapters were trimmed, residual spike-in and PhiX sequences were removed, three steps of error-correction took place, and reads were merged. These merged reads, as well as high-confidence unmerged paired-end reads that could not be grouped into an overlapping merged read, were used for SAVAGE assembly. The following workflow was implemented in a reproducible snakemake workflow that fully documents parameter selection (Koster and Rahman 2012), and is available upon request.

SAVAGE is designed to construct individual haplotypes from the overlap graph of individual reads. We processed the totality of sequence data in a single patch in order to maximize the sensitivity of the contiguous reconstruction with parameter '--split 1', as well as the parameter '--revcomp' to handle reverse complement reads. The IPD exon 2

reference database that was used for MiSeq and DSR genotyping was also used to assess the quality of SAVAGE genotypes. The IPD sequences were mapped to contigs produced by SAVAGE using sensitive parameters in bbmap (minlength=100 vslow=t subfilter=0 indelfilter=0 lengthtag=t ignorefrequentkmers=t kfilter=100) designed to identify sequences that perfectly match SAVAGE contigs. A post-processing script refined these mappings, and only retained the mappings where the length of the mapped region was the same as the length of the IPD exon 2 sequence. These mappings indicated where the reference database sequence was fully and exactly contained within a SAVAGE contig.

### **Results**

228

229

230

231

232

233

234

235

236

237

238

239

240

241

242

243

244

245

246

247

248

249

250

251

MHC reads are efficiently enriched using target-capture probes We designed a custom target enrichment probeset that accounts for the extensive duplication of macaque MHC genes (Prall et al. 2017). A tripartite target capture system was used in this study. The first component is SeqCap EZ HGSC VCRome2.1, an optimized human clinical exome probeset. Since macaques are closely related to humans, SeqCap EZ HGSC VCRome2.1 can also be used in macaques, though some sequences that are most divergent between macaques and humans are not efficiently captured. The second component of the target capture system is an additional 22,884 rhesus macaque exon sequences that were not effectively captured with the SeqCap EZ HGSC VCRome2.1 reagent. The third component is a collection of probes designed to specifically enrich macaque MHC class I and class II sequences. These probes span the full length of HLA class I and class II genes including introns, 3' UTRs, and approximately 1,000 bp of flanking 5' sequence. We obtained a median coverage of 100X for the target exon sequences across the genome with >20X coverage for 94.97% of bases that were targeted in this study. As illustrated in **Table 1**, an average of 70,549,789 Illumina sequence reads per sample were obtained for the 27 animals evaluated in this study. These reads were mapped against reference files containing representative genomic HLA exons 2 - 3 for HLA-A, and HLA-E exons 2 - 4 for HLA-DRA, -DRB1, -DRB3, -DRB4, -DRB5, -DOA1, -DOB1, -DPA1 and -DPB1 sequences. We identified an average of 269,057 MHC class I and class II sequence reads per sample which corresponds to an average of 0.37% of the total sequence reads evaluated per sample (**Table 1**). In a previous study by Ericsen et al. (Ericsen et al. 2014), we found that MHC sequences only accounted for an average of 0.13% of the total Illumina sequence reads that were evaluated per animal when the standard HGSC VCRome2.1 panel was used alone for target capture (Supplementary Table 1). Thus, we achieved an almost three-fold increase of MHC genomic sequences after inclusion of the spike-in probes for target capture compared to use of the VCRome2.1 probeset alone. MHC genotypes defined from target-enriched genomic DNA are comparable to those obtained by amplicon deep sequencing

253

254

255

256

257

258

259

260

261

262

263

264

265

266

267

268

269

270

271

272

273

274

275

276

We hypothesized that MHC genotypes derived from target-enriched genomic sequence would be comparable in accuracy to MHC genotypes derived from conventional amplicon deep sequencing. MHC class I and class II PCR amplicons were generated from the same 27 animals and deep sequenced on an Illumina MiSeq. Representative MHC class I and class II genotypes supported by the amplicon data are shown in **Figure 1** and **Figure 2**, respectively. These figures illustrate genotypes from a pedigreed family of Indian rhesus macaques: a Sire, a Dam, and three Progeny that are paternal half-siblings. Comprehensive genotypes for all 27 Indian rhesus macaques evaluated in this study are shown in **Supplementary Figure 1**. The superset of alleles supported by at least two of the methods described in this manuscript (MiSeq amplicon genotyping, DSR genotyping of individual exome sequencing reads, or SAVAGE genotyping of contigs derived from exome data), was considered to be the expected MHC genotypes for these animals. A complication for this assertion was certain genotypes were difficult for MiSeq analysis to report correctly. As we have shown previously (Karl et al. 2017), the number of reads supporting each genotyping call was highly variable, ranging from tens of reads to thousands of reads per allele. A small subset of allelic variants contained nucleotide substitutions in their sequences within the binding sites of the PCR oligonucleotides that interfere with efficient PCR amplification. This result is exemplified when members of the Mamu-B11L\*01 allele lineage were closely examined. Members of the Mamu-B11L\*01 allele lineage have two nucleotide substitutions relative to the 5' oligonucleotide that was used to generate MHC class I amplicons, so these Mamu-B11L\*01 sequences were routinely absent in MiSeq genotypes (Figure 1). Likewise, the Manu-DPA1\*11:01 allele has four nucleotide substitutions relative to the oligonucleotide pair used to generate *DPA1* amplicons for MiSeq genotyping (**Figure 2**). These nucleotide substitutions do not fully account for all differences in the abundance of sequence reads for each allele. False negatives were also noted for certain allele lineages, such as Mamu-B\*074 and Mamu-B\*098, which exhibited significantly diminished PCR efficiency despite being completely matched with the oligonucleotides used for amplification (Figure 1). False positive genotyping calls were also noted in the MiSeq assay that resulted from intermolecular recombination during the PCR process. This was exemplified by read support for the presence of Mamu-B\*007:07 in Sire r07010, and Progeny 2 r17041 (Figure 1). Mamu-B\*007:07 only differs from the Mamu-

278

279

280

281

282

283

284

285

286

287

288

289

290

291

292

293

294

295

296

297

298

299

300

301

B\*007g1 allele group that was determined to be present in this pair of animals by a single nucleotide variant at the extreme 5' end of the class I genotyping amplicon. Chimeric PCR products equivalent to the Mamu-B\*007:07 sequence were formed between the 3' portion of the Mamu-B\*007g1 sequence and other allelic variants in these animals with this 5' SNP. Taken together, these results illustrate that the MiSeq amplicon genotyping, while generally reflective of an animal's MHC genotype, can yield both false positive and false negative results. When compared to the expected genotypes for this dataset, MiSeq amplicon genotyping has 90.4% MHC class I and 97.8% MHC class II concordance (**Table 2**). Two separate strategies were used to derive MHC genotypes from target-capture data. The DSR analysis was a straightforward extension of the methodology used for deriving genotypes from MiSeq amplicons. MHC sequence reads were extracted from the total exome dataset. A simplified workflow that mapped those MHC reads to reference sequences, and then assigned the genotypes based on the presence of exome reads overlapping each position of the reference sequence, was problematic. This simplified workflow was extremely vulnerable to false positive genotypes, and the similarities among different MHC sequences often enabled those reads to map to multiple different alleles (Wiseman et al. 2013). Two or more reads each could partially match a portion of a sequence in the IPD exon 2 database, which could complement each other to provide support for an allele that was not biologically relevant. As discussed in the Methods, the DSR encompassed polymorphisms that discriminated among closely related alleles by requiring at least one mapped read to unambiguously map to the corresponding allele within the IPD exon 2 sequences. This strategy can identify specific polymorphisms of interest among the IPD exon 2 sequences to produce genotypes for MHC class I and MHC class II (Figures 1, 2 and Supplementary Figure 1). For the 27 animals evaluated in this study, DSR was 97.3% and 100% concordant with expected MHC class I and class II genotypes, respectively (Table 2). The DSR strategy did not consider sequences that were not among the IPD exon 2 sequences and this lack of consideration contributes to overcalled alleles. The apparent Mamu-A1\*059:01 allele in Dam r05029 was erroneously derived from reads that were from Mamu-A1\*004g1 and an unknown allele that was not among the sequences in the IPD exon 2 database. As a result of this unknown sequence not being among the known IPD exon

303

304

305

306

307

308

309

310

311

312

313

314

315

316

317

318

319

320

321

2 sequences, reads unambiguously mapped to Mamu-A1\*059:01, which caused this allele to be overcalled. This type of overcalling will be mitigated with the discovery of additional allelic variants, and their inclusion in future iterations of the IPD database. The second approach for determining genotypes performed de novo assembly on MHC class I and class II reads from each sample. The resulting assembled contigs were then mapped against IPD exon 2 reference sequences to define perfectly matching contigs. Because most assemblers were not tuned for the challenge of assembling large numbers of contigs that differ from one another by as little as 1 bp, we relied on an assembler, SAVAGE, originally designed to reconstruct viral sequencing haplotypes. As shown in Figures 1, 2 and Supplementary Figure 1, contigs produced by SAVAGE matched the expected genotypes. Unlike the DSR method, SAVAGE assembled contigs for downstream analyses. False positives and false negatives among closely-related variants were mitigated by the inclusion of the filtering steps described under Strategy 2. Across all 27 samples, the SAVAGE contigs are 98.3% and 99.7% accurate with respect to the expected MHC genotypes (Table 2). While this analysis focused on genotyping using the same exon 2 reference sequences that are commonly utilized for MiSeq amplicon analyses, the SAVAGE contigs are frequently much longer than these reference sequences (Figure 3). These extended contigs frequently contain exons 2 through 4, plus the intervening introns, and could be used to provide higher resolution genotyping than is possible using exon 2 sequence alone. Moreover, contigs that contain complete sequences for exons 2-3 of MHC class I and exon 2 of MHC class II alleles meet the minimum criteria for obtaining formal allele nomenclature for non-human primates from the IPD-MHC (Robinson et al. 2013).

### **Discussion**

322

323

324

325

326

327

328

329

330

331

332

333

334

335

336

337

338

339

340

341

342

343

344

345

346

347

Here we describe MES genotyping of Indian rhesus macaques. In our estimation, this method will supersede MiSeq PCR amplicon genotyping as the most widely used macaque MHC genotyping assay in the future. This methodology has a number of compelling advantages. Most importantly, exome sequencing dramatically improves the overall quantity and quality of genomic information obtained from each sample. The same datasets used for MHC analyses may be used to evaluate protein-coding genetic variation throughout the genome. The loss of start and stop codons exome-wide can be obtained from the same datasets by modifying the workflows in silico, as opposed to requiring the sequencing of multiple new sets of target genes (Yang et al. 2013). Exome-wide datasets offer the promise of retrospectively identifying candidate DNA sequence variants that may be responsible for unexpected experimental outcomes in studies with macaques and other nonhuman primates. The availability of exome-wide sequences in conjunction with MHC genotypes may also increase the rigor of prospective macaque experiments by enabling more sophisticated balancing of experimental groups, and exclusion of animals whose genetics are likely to strongly bias experimental results (Loffredo et al. 2007; Reynolds et al. 2011; Haus et al. 2014). These same exome datasets also offer the potential to improve the quality of MHC genotyping. Full-length long-read MHC transcript sequencing offers exquisite resolution, but this technology can be labor intensive and difficult to scale (Karl et al. 2017; Semler et al. 2018). The MiSeq exon 2 amplicon approach is limited in its allelic resolution, but it is the current standard deep sequencing approach for high-throughput MHC genotyping in macaques. In this report, we compare two novel strategies for MHC genotyping from MES datasets to this standard MiSeq amplicon genotyping method. The results that we obtained with all three approaches show strong concordance with expected MHC genotypes for the Indian rhesus macaques that were evaluated. As illustrated in Figure 3a, MHC class I genomic contigs with an average length of approximately 1.1 kb can be assembled from sequence reads that were initially extracted from the whole exome datasets. Following the initial enrichment step, MHC class II genomic contigs averaging approximately 1.9 kb in length could be assembled from whole exome sequence reads that mapped to HLA-DRB1,-DRB4, -DRB5, -DQA1, -DQB1, -DPA1 and -DPB1 reference sequences, which contained exons 2 - 4, and the pairs of introns (Figure 3b). The

349

350

351

352

353

354

355

356

357

358

359

360

361

362

363

364

365

366

367

368

369

370

371

372

addition of HLA spike-in probes containing both exon and intron sequences for the target capture step, and the introduction of 151 bp paired end reads for the Illumina NovaSeq platform greatly facilitated our ability to assemble these extended MHC genomic contigs. Additional technological advances, including even longer sequence reads and more efficient assembly algorithms, will undoubtedly increase genomic contig lengths as well as MHC allelic resolution in future studies. Both MHC genotyping approaches described here depend upon mapping exome sequence reads against a reference database of MHC class I and class II allele sequences. Currently, the IPD database essentially is restricted to coding regions for macaque MHC sequences, and many IPD entries are only partial transcript sequences that lack complete coding regions. In addition, it is very challenging to correctly phase short Illumina sequence read that map to different exons of a specific allelic variant and are separated by intronic sequences that span hundreds to thousands of base pairs in genomic DNA. Our results with the SAVAGE workflow (Figure 3) demonstrate that exome sequence reads that have been enriched with the enhanced MHC probe design described here can be assembled into genomic contigs that span multiple exons and introns. These contigs, therefore, could also be used to improve MHC reference databases, though this requires a major effort with more animals, and is beyond the scope of this manuscript. The current cost of genotyping is relatively high compared to amplicon deep sequencing, largely due to two expenses. First, the amount of sequence data needed for a single sample can be high. Compared to conventional MHC genotyping, where 192 macaques' data can be collected on a single instrument run, exome data acquisition is much more expensive. On an Illumina Novaseq instrument, which has a much higher run cost than the MiSeq, only 70 exome samples can be sequenced simultaneously per lane of a S4 flow cell. However, this cost of sequencing is rapidly decreasing, and as of early 2019, commercial providers have advertised sequencing for \$9 USD per Gb of whole genome sequence data<sup>1</sup>. Second, a major expense in MHC genotyping is the production, validation, and use of target-capture arrays, as well as the development of in silico data analysis workflows. The approaches described here, in particular MHC genotyping from SAVAGE contigs produced by de novo assembly of exome reads, is flexible and should be adaptable as sequencing approaches evolve and improve.

<sup>1</sup> Comment via Twitter 03/18/2019 @albertvilella https://twitter.com/AlbertVilella/status/1107524501645000705

A major goal for future studies will be to attempt to extend these contigs to encompass full length genomic MHC sequences using SAVAGE or other assembly software tools. The relatively compact genomic structure and consistent length of MHC class I genes increase the attainability of this goal. Establishment of comprehensive macaque MHC allele databases of extended genomic sequences will greatly facilitate mapping of exome sequence reads since they will be contiguous with the reference sequences instead of being interrupted by intervening sequences between each exon that are not included in current non-human primate IPD-MHC databases (Maccari et al. 2017).

These results demonstrate that MHC genotypes can be obtained by analyzing genomic DNA selectively enriched for MHC and protein-coding gene sequences. This represents an important advance for characterizing MHC genetics in macaques, and this suggests that analyses of whole exome and whole genome data will become the predominant method for studying macaque genetics in the coming decade.

Acknowledgements

We gratefully acknowledge Michele Di Mascio and his group at the National Institute of Allergy and Infectious Diseases of the National Institutes of Health for providing rhesus macaque samples used in this study. We also gratefully thank Brian Bushnell for assistance with the BBTools software, and the WNPRC for providing samples from five related macaques. This research was supported by contracts HHSN272201600007C from the National Institute of Allergy and Infectious Diseases of the National Institutes of Health. This work was also supported in part by the Office of Research Infrastructure Programs/OD (P510D011106) awarded to the Wisconsin National Primate Research Center at the University of Wisconsin-Madison. This research was also supported in part by grant R24-OD011173 from the National Institutes of Health. This research was conducted in part at a facility constructed with support from Research Facilities Improvement Program grants RR15459-01 and RR020141-01.

#### **Figure Legends**

405

406

407

408

409

410

411

412

413

414

415

416

417

418

419

420

421

422

423

424

425

426

427

428

429

**Table 1.** Fraction of total exome sequence reads corresponding to exons 2 - 3 of MHC class I and exons 2 - 4 of MHC class II genes. **Table 2.** Summary of discordant results for each MHC genotyping method by animal. Figure 1. Comparison of MHC class I results from MiSeq PCR amplicon versus whole exome genotyping strategies for a representative breeding group of rhesus macaques. Results for each of the three methods are provided side-byside in the columns for each macaque. Each row indicates the detection of a specific MHC class I allele or lineage group of closely related sequences that are ambiguous because they are identical over the IPD exon 2 database sequence. Values in the body of this figure indicate the number of sequence reads supporting each allele call for the MiSeq and DSR methods while alleles supported by a SAVAGE contig are reported with a "1". Discrepancies between the MiSeq (pink), DSR (yellow) or SAVAGE (blue) methods are highlighted by filled cells with borders. Figure 2. Comparison of MHC class II results from MiSeq PCR amplicon versus whole exome genotyping strategies for a representative breeding group of rhesus macaques. Results for each of the three methods are provided side-by-side in the columns for these five related macaques. Each row indicates detection of a specific MHC class II allele or lineage group of closely related sequences that are ambiguous because they are identical over the IPD exon 2 database sequence. Values in the body of this figure indicate the number of sequence reads supporting each allele call for the MiSeq and DSR methods while alleles supported by a SAVAGE contig are reported with a "1". The Mamu-DPA1\*11:01 allele missed by the MiSeq assay due to multiple mismatches versus the amplification primers is highlighted in pink. Figure 3. Lengths of MHC sequence contigs assembled by the SAVAGE method for a representative breeding group of rhesus macaques. Values in the body of this figure indicate contig lengths generated for these MHC sequences in each animal. (A) MHC class I genotyping results are illustrated for the five animals in this breeding group. Three false negative allele calls for SAVAGE versus the expected genotypes for these animals are highlighted in magenta, e.g., Mamu-B\*030g1 in Sire r07010. Sequences highlighted in red are associated with the maternal MHC Haplotype a that was inherited by Progeny 1 from its Dam. Sequences in Progeny 1 and Progeny 3

for their MHC Haplotype b that was inherited from Sire r07010 are highlighted in dark blue while the light blue sequences represent the alternate paternal Haplotype c that was inherited by Progeny 2. Three unique extended MHC Haplotypes in this breeding group are indicated with shades of grey (Haplotypes d - f). MHC allele groups that are shared by both parental haplotypes are indicated by colored borders around filled cells. (**B**) MHC class II genotyping results are illustrated for this same breeding group. (**C**) Abbreviated Mamu haplotype designations (Karl et al. 2013) are summarized for the six extended MHC haplotypes identified by segregation in this breeding group. For example, the twenty MHC sequences (red) that are associated with extended Haplotype a can be summarized by the following string of abbreviated Mamu haplotype designations: Mamu-A004/B048/DR04a/DQA01g1/DQB06:01/DPA02g1/DPB15g.

**Supplementary Materials** 

Supplementary Table 1. Fraction of total exome sequence reads corresponding to MHC class I and class II genes after target capture with the VCRome2.1 probe design alone. This exome sequence dataset was described previously by Ericsen and coworkers (Ericsen et al. 2014).

Supplementary Figure 1. Comparison of MHC class I results from MiSeq PCR amplicon versus whole exome genotyping assays with the DSR and SAVAGE strategies for all 27 animals. Results for each of the three method are provided side-by-side in the columns for each macaque. Each row indicates the detection of a specific MHC class I allele or lineage group of closely related sequences that are ambiguous because they are identical over the IPD exon 2 database sequence. Values in the body of this figure indicate the number of sequence reads supporting each allele call for the MiSeq and DSR methods while alleles supported by a SAVAGE contig are reported with a "1".

Discrepancies between the MiSeq (pink), DSR (yellow) or SAVAGE (blue) methods are highlighted by filled cells with borders.

#### References

457

458

459

460

461

462

463

464

465

466

467

468

469

470

471

472

473

474

475

476

477

478

479

480

481

482

483

Animal Welfare Act. 'The Animal Welfare Act - Public Law 89-544 Act of August 24, 1966, 1966. https://www.nal.usda.gov/awic/animal-welfare-act-public-law-89-544-act-august-24-1966. Accessed 05/01/2019 Baaijens, J. A., A. Z. E. Aabidine, E. Rivals, and A. Schonhuth. 2017. De novo assembly of viral quasispecies using overlap graphs. Genome Res 27: 835-848. https://www.ncbi.nlm.nih.gov/pubmed/28396522 Bimber, B. N., R. Ramakrishnan, R. Cervera-Juanes, R. Madhira, S. M. Peterson, R. B. J. Norgren, and B. Ferguson. 2017. Whole genome sequencing predicts novel human disease models in rhesus macaques. *Genomics* 109: 214-220. https://www.ncbi.nlm.nih.gov/pubmed/28438488 Brown, J. H., T. S. Jardetzky, J. C. Gorga, L. J. Stern, R. G. Urban, J. L. Strominger, and D. C. Wiley. 1993. Threedimensional structure of the human class II histocompatibility antigen HLA-DR1. Nature 364: 33-39. https://www.ncbi.nlm.nih.gov/pubmed/8316295 Bushnell, B., J. Rood, and E. Singer. 2017. BBMerge - Accurate paired shotgun read merging via overlap. PLoS One 12: e0185056. https://www.ncbi.nlm.nih.gov/pubmed/29073143 Cao, H., J. Wu, Y. Wang, H. Jiang, T. Zhang, X. Liu, Y. Xu, D. Liang, P. Gao, Y. Sun, B. Gifford, M. D'Ascenzo, X. Liu, L. C. Tellier, F. Yang, X. Tong, D. Chen, J. Zheng, W. Li, T. Richmond, X. Xu, J. Wang, and Y. Li. 2013. An integrated tool to study MHC region: accurate SNV detection and HLA genes typing in human MHC region using targeted high-throughput sequencing. PLoS One 8: e69388. https://www.ncbi.nlm.nih.gov/pubmed/23894464 Clark, M. J., R. Chen, and M. Snyder. 2013. Exome sequencing by targeted enrichment. Curr Protoc Mol Biol Chapter 7: Unit7.12. https://www.ncbi.nlm.nih.gov/pubmed/23547016 Cornish, A. S., R. M. Gibbs, and R. B. J. Norgren. 2016. Exome screening to identify loss-of-function mutations in the rhesus macaque for development of preclinical models of human disease. BMC Genomics 17: 170. https://www.ncbi.nlm.nih.gov/pubmed/26935327 Daza-Vamenta, R., G. Glusman, L. Rowen, B. Guthrie, and D. E. Geraghty. 2004. Genetic divergence of the rhesus macaque major histocompatibility complex. Genome Res 14: 1501-1515. https://www.ncbi.nlm.nih.gov/pubmed/15289473

484 de Manuel, M., T. Shiina, S. Suzuki, N. Dereuddre-Bosquet, H. J. Garchon, M. Tanaka, N. Congy-Jolivet, A. 485 Aarnink, R. Le Grand, T. Marques-Bonet, and A. Blancher. 2018. Whole genome sequencing in the search 486 for genes associated with the control of SIV infection in the Mauritian macaque model. Sci Rep 8: 7131. 487 https://www.ncbi.nlm.nih.gov/pubmed/29739964 488 Edgar, R. C. 2010. Search and clustering orders of magnitude faster than BLAST. Bioinformatics 26: 2460-2461. 489 https://www.ncbi.nlm.nih.gov/pubmed/20709691 490 Ericsen, A. J., G. J. Starrett, J. M. Greene, M. Lauck, M. Raveendran, D. R. Deiros, M. S. Mohns, N. Vince, B. T. 491 Cain, N. H. Pham, J. T. Weinfurter, A. L. Bailey, M. L. Budde, R. W. Wiseman, R. Gibbs, D. Muzny, T. C. 492 Friedrich, J. Rogers, and D. H. O'Connor. 2014. Whole genome sequencing of SIV-infected macaques 493 identifies candidate loci that may contribute to host control of virus replication. Genome Biol 15: 478. 494 https://www.ncbi.nlm.nih.gov/pubmed/25418588 495 Garcia, K. C., and E. J. Adams. 2005. How the T cell receptor sees antigen--a structural view. Cell 122: 333-336. 496 https://www.ncbi.nlm.nih.gov/pubmed/16096054 497 Haus, T., B. Ferguson, J. Rogers, G. Doxiadis, U. Certa, N. J. Rose, R. Teepe, G. F. Weinbauer, and C. Roos. 2014. 498 Genome typing of nonhuman primate models: implications for biomedical research. Trends Genet 30: 482-499 487. https://www.ncbi.nlm.nih.gov/pubmed/24954183 500 Horton, R., R. Gibson, P. Coggill, M. Miretti, R. J. Allcock, J. Almeida, S. Forbes, J. G. Gilbert, K. Halls, J. L. 501 Harrow, E. Hart, K. Howe, D. K. Jackson, S. Palmer, A. N. Roberts, S. Sims, C. A. Stewart, J. A. Traherne, 502 S. Trevanion, L. Wilming, J. Rogers, P. J. de Jong, J. F. Elliott, S. Sawcer, J. A. Todd, J. Trowsdale, and S. 503 Beck. 2008. Variation analysis and gene annotation of eight MHC haplotypes: the MHC Haplotype Project. 504 Immunogenetics 60: 1-18. https://www.ncbi.nlm.nih.gov/pubmed/18193213 505 Kaizu, M., G. J. Borchardt, C. E. Glidden, D. L. Fisk, J. T. Loffredo, D. I. Watkins, and W. M. Rehrauer. 2007. 506 Molecular typing of major histocompatibility complex class I alleles in the Indian rhesus macaque which 507 restrict SIV CD8+ T cell epitopes. *Immunogenetics* 59: 693-703. 508 https://www.ncbi.nlm.nih.gov/pubmed/17641886 509 Karl, J. A., P. S. Bohn, R. W. Wiseman, F. A. Nimityongskul, S. M. Lank, G. J. Starrett, and D. H. O'Connor. 2013. 510 Major histocompatibility complex class I haplotype diversity in Chinese rhesus macaques. G3 (Bethesda) 3:

1195-1201. https://www.ncbi.nlm.nih.gov/pubmed/23696100

511

513

514

515

516

517

518

519

520

521

522

523

524

525

526

527

528

529

530

531

532

533

534

535

536

537

538

539

Karl, J. A., M. E. Graham, R. W. Wiseman, K. E. Heimbruch, S. M. Gieger, G. G. Doxiadis, R. E. Bontrop, and D. H. O'Connor. 2017. Major histocompatibility complex haplotyping and long-amplicon allele discovery in cynomolgus macaques from Chinese breeding facilities. *Immunogenetics* 69: 211-229. https://www.ncbi.nlm.nih.gov/pubmed/28078358 Karl, J. A., K. E. Heimbruch, C. E. Vriezen, C. J. Mironczuk, D. M. Dudley, R. W. Wiseman, and D. H. O'Connor. 2014. Survey of major histocompatibility complex class II diversity in pig-tailed macaques. *Immunogenetics* 66: 613-623. https://www.ncbi.nlm.nih.gov/pubmed/25129472 Kishikawa, T., Y. Momozawa, T. Ozeki, T. Mushiroda, H. Inohara, Y. Kamatani, M. Kubo, and Y. Okada. 2019. Empirical evaluation of variant calling accuracy using ultra-deep whole-genome sequencing data. Sci Rep 9: 1784. https://www.ncbi.nlm.nih.gov/pubmed/30741997 Koster, J., and S. Rahmann. 2012. Snakemake--a scalable bioinformatics workflow engine. Bioinformatics 28: 2520-2522. https://www.ncbi.nlm.nih.gov/pubmed/22908215 Loffredo, J. T., J. Maxwell, Y. Oi, C. E. Glidden, G. J. Borchardt, T. Soma, A. T. Bean, D. R. Beal, N. A. Wilson, W. M. Rehrauer, J. D. Lifson, M. Carrington, and D. I. Watkins. 2007. Mamu-B\*08-positive macaques control simian immunodeficiency virus replication. J Virol 81: 8827-8832. https://www.ncbi.nlm.nih.gov/pubmed/17537848 Loffredo, J. T., J. Sidney, A. T. Bean, D. R. Beal, W. Bardet, A. Wahl, O. E. Hawkins, S. Piaskowski, N. A. Wilson, W. H. Hildebrand, D. I. Watkins, and A. Sette. 2009. Two MHC class I molecules associated with elite control of immunodeficiency virus replication, Mamu-B\*08 and HLA-B\*2705, bind peptides with sequence similarity. J Immunol 182: 7763-7775. https://www.ncbi.nlm.nih.gov/pubmed/19494300 Maccari, G., J. Robinson, K. Ballingall, L. A. Guethlein, U. Grimholt, J. Kaufman, C. S. Ho, N. G. de Groot, P. Flicek, R. E. Bontrop, J. A. Hammond, and S. G. Marsh. 2017. IPD-MHC 2.0: an improved inter-species database for the study of the major histocompatibility complex. Nucleic Acids Res 45: D860-D864. https://www.ncbi.nlm.nih.gov/pubmed/27899604 Malissen, M., B. Malissen, and B. R. Jordan. 1982. Exon/intron organization and complete nucleotide sequence of an HLA gene. Proc Natl Acad Sci USA 79: 893-897. https://www.ncbi.nlm.nih.gov/pubmed/6461010 Mothe, B. R., J. Weinfurter, C. Wang, W. Rehrauer, N. Wilson, T. M. Allen, D. B. Allison, and D. I. Watkins. 2003. Expression of the major histocompatibility complex class I molecule Mamu-A\*01 is associated with control

540 of simian immunodeficiency virus SIVmac239 replication. J Virol 77: 2736-2740. 541 https://www.ncbi.nlm.nih.gov/pubmed/12552014 Muhl, T., M. Krawczak, P. Ten Haaft, G. Hunsmann, and U. Sauermann, 2002, MHC class I alleles influence set-542 543 point viral load and survival time in simian immunodeficiency virus-infected rhesus monkeys. J Immunol 544 169: 3438-3446. https://www.ncbi.nlm.nih.gov/pubmed/12218167 545 Nomura, T., H. Yamamoto, T. Shiino, N. Takahashi, T. Nakane, N. Iwamoto, H. Ishii, T. Tsukamoto, M. Kawada, 546 S. Matsuoka, A. Takeda, K. Terahara, Y. Tsunetsugu-Yokota, N. Iwata-Yoshikawa, H. Hasegawa, T. Sata, T. 547 K. Naruse, A. Kimura, and T. Matano. 2012. Association of major histocompatibility complex class I 548 haplotypes with disease progression after simian immunodeficiency virus challenge in burmese rhesus 549 macaques. J Virol 86: 6481-6490. https://www.ncbi.nlm.nih.gov/pubmed/22491464 550 Otting, N., M. K. van der Wiel, N. de Groot, A. J. de Vos-Rouweler, N. G. de Groot, G. G. Doxiadis, R. W. 551 Wiseman, D. H. O'Connor, and R. E. Bontrop. 2017. The orthologs of HLA-DQ and -DP genes display 552 abundant levels of variability in macague species. *Immunogenetics* 69: 87-99. 553 https://www.ncbi.nlm.nih.gov/pubmed/27771735 Posey, J. E., J. A. Rosenfeld, R. A. James, M. Bainbridge, Z. Niu, X. Wang, S. Dhar, W. Wiszniewski, Z. H. 554 555 Akdemir, T. Gambin, F. Xia, R. E. Person, M. Walkiewicz, C. A. Shaw, V. R. Sutton, A. L. Beaudet, D. 556 Muzny, C. M. Eng, Y. Yang, R. A. Gibbs, J. R. Lupski, E. Boerwinkle, and S. E. Plon. 2016. Molecular 557 diagnostic experience of whole-exome sequencing in adult patients. Genet Med 18: 678-685. 558 https://www.ncbi.nlm.nih.gov/pubmed/26633545 559 Prall, T. M., M. E. Graham, J. A. Karl, R. W. Wiseman, A. J. Ericsen, M. Raveendran, R. Alan Harris, D. M. 560 Muzny, R. A. Gibbs, J. Rogers, and D. H. O'Connor. 2017. Improved full-length killer cell immunoglobulinlike receptor transcript discovery in Mauritian cynomolgus macaques. Immunogenetics 69: 325-339. 561 562 https://www.ncbi.nlm.nih.gov/pubmed/28343239 Revnolds, M. R., J. B. Sacha, A. M. Weiler, G. J. Borchardt, C. E. Glidden, N. C. Sheppard, F. A. Norante, P. A. 563 564 Castrovinci, J. J. Harris, H. T. Robertson, T. C. Friedrich, A. B. McDermott, N. A. Wilson, D. B. Allison, W. C. Koff, W. E. Johnson, and D. I. Watkins. 2011. The TRIM5 (alpha) genotype of rhesus macaques affects 565 566 acquisition of simian immunodeficiency virus SIVsmE660 infection after repeated limiting-dose intrarectal 567 challenge. J Virol 85: 9637-9640. https://www.ncbi.nlm.nih.gov/pubmed/21734037

569

570

571

572

573

574

575

576

577

578

579

580

581

582

583

584

585

586

587

588

589

590

591

592

593

594

https://www.ncbi.nlm.nih.gov/pubmed/25753671

Robinson, J., J. A. Halliwell, H. McWilliam, R. Lopez, and S. G. Marsh. 2013. IPD--the Immuno Polymorphism Database. Nucleic Acids Res 41: D1234-40. https://www.ncbi.nlm.nih.gov/pubmed/23180793 Semler, M. R., R. W. Wiseman, J. A. Karl, M. E. Graham, S. M. Gieger, and D. H. O'Connor, 2018, Novel fulllength major histocompatibility complex class I allele discovery and haplotype definition in pig-tailed macaques. Immunogenetics 70: 381-399. https://www.ncbi.nlm.nih.gov/pubmed/29134258 Shiina, T., A. Blancher, H. Inoko, and J. K. Kulski. 2017. Comparative genomics of the human, macaque and mouse major histocompatibility complex. *Immunology* 150: 127-138. https://www.ncbi.nlm.nih.gov/pubmed/27395034 Silver, Z. A., and D. I. Watkins. 2017. The role of MHC class I gene products in SIV infection of macaques. Immunogenetics 69: 511-519. https://www.ncbi.nlm.nih.gov/pubmed/28695289 Vallender, E. J. 2011. Expanding whole exome resequencing into non-human primates. Genome Biol 12: R87. https://www.ncbi.nlm.nih.gov/pubmed/21917143 Weatherall, D. 2006. The use of non-human primates in research, 147, https://mrc.ukri.org/documents/pdf/the-useof-non-human-primates-in-research/. Accessed 04/30/2019 Williams, T. M. 2001. Human leukocyte antigen gene polymorphism and the histocompatibility laboratory. J Mol Diagn 3: 98-104. https://www.ncbi.nlm.nih.gov/pubmed/11486048 Wiseman, R. W., J. A. Karl, B. N. Bimber, C. E. O'Leary, S. M. Lank, J. J. Tuscher, A. M. Detmer, P. Bouffard, N. Levenkova, C. L. Turcotte, E. J. Szekeres, C. Wright, T. Harkins, and D. H. O'Connor. 2009. Major histocompatibility complex genotyping with massively parallel pyrosequencing. Nat Med 15: 1322-1326. https://www.ncbi.nlm.nih.gov/pubmed/19820716 Wiseman, R. W., J. A. Karl, P. S. Bohn, F. A. Nimityongskul, G. J. Starrett, and D. H. O'Connor. 2013. Haplessly hoping: macaque major histocompatibility complex made easy. ILAR J 54: 196-210. https://www.ncbi.nlm.nih.gov/pubmed/24174442 Wittig, M., J. A. Anmarkrud, J. C. Kassens, S. Koch, M. Forster, E. Ellinghaus, J. R. Hov, S. Sauer, M. Schimmler, M. Ziemann, S. Gorg, F. Jacob, T. H. Karlsen, and A. Franke. 2015. Development of a high-resolution NGSbased HLA-typing and analysis pipeline. *Nucleic Acids Res* 43: e70.

596

597

598

599

600

601

602

603

604

605

606

607

608

609

610

611

612

613

614

615

616

617

618

619

620

621

Xie, C., Z. X. Yeo, M. Wong, J. Piper, T. Long, E. F. Kirkness, W. H. Biggs, K. Bloom, S. Spellman, C. Vierra-Green, C. Brady, R. H. Scheuermann, A. Telenti, S. Howard, S. Brewerton, Y. Turpaz, and J. C. Venter. 2017. Fast and accurate HLA typing from short-read next-generation sequence data with xHLA. Proc Natl Acad Sci U S A 114: 8059-8064. https://www.ncbi.nlm.nih.gov/pubmed/28674023 Xue, C., M. Raveendran, R. A. Harris, G. L. Fawcett, X. Liu, S. White, M. Dahdouli, D. Rio Deiros, J. E. Below, W. Salerno, L. Cox, G. Fan, B. Ferguson, J. Horvath, Z. Johnson, S. Kanthaswamy, H. M. Kubisch, D. Liu, M. Platt, D. G. Smith, B. Sun, E. J. Vallender, F. Wang, R. W. Wiseman, R. Chen, D. M. Muzny, R. A. Gibbs, F. Yu, and J. Rogers. 2016. The population genomics of rhesus macaques (Macaca mulatta) based on wholegenome sequences. Genome Res 26: 1651-1662. https://www.ncbi.nlm.nih.gov/pubmed/27934697 Yang, Y., D. M. Muzny, J. G. Reid, M. N. Bainbridge, A. Willis, P. A. Ward, A. Braxton, J. Beuten, F. Xia, Z. Niu, M. Hardison, R. Person, M. R. Bekheirnia, M. S. Leduc, A. Kirby, P. Pham, J. Scull, M. Wang, Y. Ding, S. E. Plon, J. R. Lupski, A. L. Beaudet, R. A. Gibbs, and C. M. Eng. 2013. Clinical whole-exome sequencing for the diagnosis of mendelian disorders. N Engl J Med 369: 1502-1511. https://www.ncbi.nlm.nih.gov/pubmed/24088041 Yang, Y., D. M. Muzny, F. Xia, Z. Niu, R. Person, Y. Ding, P. Ward, A. Braxton, M. Wang, C. Buhay, N. Veeraraghavan, A. Hawes, T. Chiang, M. Leduc, J. Beuten, J. Zhang, W. He, J. Scull, A. Willis, M. Landsverk, W. J. Craigen, M. R. Bekheirnia, A. Stray-Pedersen, P. Liu, S. Wen, W. Alcaraz, H. Cui, M. Walkiewicz, J. Reid, M. Bainbridge, A. Patel, E. Boerwinkle, A. L. Beaudet, J. R. Lupski, S. E. Plon, R. A. Gibbs, and C. M. Eng. 2014. Molecular findings among patients referred for clinical whole-exome sequencing. JAMA 312: 1870-1879. https://www.ncbi.nlm.nih.gov/pubmed/25326635 Zimin, A. V., A. S. Cornish, M. D. Maudhoo, R. M. Gibbs, X. Zhang, S. Pandey, D. T. Meehan, K. Wipfler, S. E. Bosinger, Z. P. Johnson, G. K. Tharp, G. Marcais, M. Roberts, B. Ferguson, H. S. Fox, T. Treangen, S. L. Salzberg, J. A. Yorke, and R. B. J. Norgren. 2014. A new rhesus macaque assembly and annotation for nextgeneration sequencing analyses. Biol Direct 9: 20. https://www.ncbi.nlm.nih.gov/pubmed/25319552

Table 1. Fraction of total exome sequence reads corresponding to exons 2 - 3 of MHC class I and exons 2 - 4 of MHC class II genes

			MHC-I	DRB1/3/4/5	DQA1	DQB1	DPA1	DPB1	MHC	
		<b>Total Raw</b>	Reads	Reads	Reads	Reads	Reads	Reads	Reads	MHC %
<b>Animal ID</b>	SRA Accession	Reads	Extracted	Extracted	Extracted	Extracted	Extracted	Extracted	Extracted	of total
r05029	SAMN11131055	87,345,430	79,712	215,654	24,266	39,188	29,604	112,376	500,800	0.57
r17099	SAMN11131056	67,632,236	32,406	89,946	9,694	16,782	11,214	47,974	208,016	0.31
r07010	SAMN11173514	81,062,856	71,694	204,352	22,528	38,382	25,392	111,626	473,974	0.58
r17041	SAMN11131058	80,004,430	30,852	244,326	9,746	16,310	12,644	151,376	465,254	0.58
r17061	SAMN11131059	78,428,820	70,082	204,694	20,776	41,018	19,440	95,538	451,548	0.58
J8R	SAMN11282383	80,868,782	45,164	87,864	11,878	19,736	13,810	57,146	235,598	0.29
J01	SAMN11282382	61,009,650	34,342	87,124	9,050	16,628	10,958	46,964	205,066	0.34
ZC08	SAMN11282384	60,693,394	31,168	81,586	10,392	15,660	10,172	45,748	194,726	0.32
DGKG	SAMN11282378	80,530,772	48,658	130,256	12,788	22,682	13,372	62,990	290,746	0.36
CF18	SAMN11282368	68,593,710	37,792	96,842	10,864	18,226	13,118	51,556	228,398	0.33
DE1AA	SAMN11282369	65,712,570	39,334	108,002	10,060	17,124	11,840	51,134	237,494	0.36
DEG8	SAMN11282370	68,490,344	35,566	116,824	10,404	19,278	12,294	55,086	249,452	0.36
DEXX	SAMN11282371	67,451,626	33,900	128,128	10,442	18,898	9,778	53,258	254,404	0.38
DF24	SAMN11282372	67,768,724	41,362	96,172	10,606	18,176	10,976	50,612	227,904	0.34
DF64	SAMN11282373	65,762,818	37,426	107,974	11,222	15,632	11,446	51,214	234,914	0.36
DF6T	SAMN11282374	71,472,222	41,160	101,102	11,052	18,794	13,492	51,626	237,226	0.33
DFET	SAMN11282375	77,040,660	49,068	128,862	12,588	20,952	12,586	58,238	282,294	0.37
DFV0	SAMN11282377	73,877,184	41,924	98,866	11,630	17,690	13,952	52,394	236,456	0.32
DJ94	SAMN11282379	66,051,412	39,616	88,196	9,910	15,892	10,978	45,972	210,564	0.32
HIH	SAMN11282380	76,491,578	41,308	85,732	11,148	18,366	14,102	50,746	221,402	0.29
DFJT	SAMN11282376	62,249,064	37,728	78,860	9,666	15,268	11,426	43,086	196,034	0.31
HLJ	SAMN11282381	68,288,558	41,748	94,570	9,960	17,240	12,756	48,356	224,630	0.33
37360	SAMN11282363	62,310,824	38,200	97,452	9,866	15,024	10,320	46,140	217,002	0.35
0L7	SAMN11282364	64,145,834	35,302	128,778	9,310	19,992	10,686	54,196	258,264	0.40
0R1	SAMN11282365	64,789,208	36,462	86,772	10,656	17,258	11,982	46,124	209,254	0.32
0R8	SAMN11282366	72,836,490	38,286	118,184	10,500	22,248	13,170	56,142	258,530	0.35
0TI	SAMN11282367	80,730,750	41,552	106,356	13,364	20,714	14,860	57,744	254,590	0.32
	Average	70,549,789	42,660	119,018	12,014	20,487	13,569	61,310	269,057	0.37

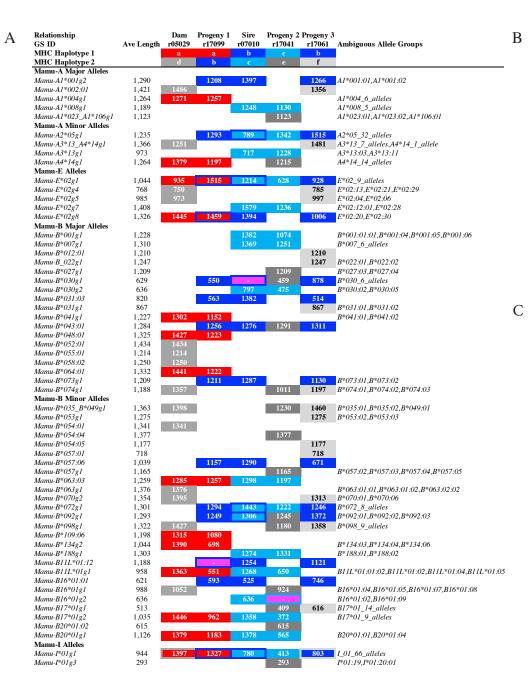
		MHC cla	ass I		MHC class II						
Animal ID	Total Alleles Expected	# MiSeq Discordance	# DSR Discordance	# SAVAGE Discordance	Total Alleles Expected	# MiSeq Discordance	# DSR Discordance	# SAVAGE Discordance			
r05029	28	2	1		10						
r17099	25	3		1	12						
r07010	26	3	1	1	12						
r17041	31	3		1	10						
r17061	29	1	2		12	1					
J8R	29	4	1		12	2					
J01	30	3	1	1	11	1					
ZC08	24	2		1	12						
DGKG	28	4	1		13						
CF18	28	3	-		12						
DE1AA	30	5	1		13						
DEG8	27	3	1		13						
DEXX	24	3	1	1	14						
DF24	32	4	•	1	12						
DF64	30	3	1	1	13						
DF6T	31	2	•	1	10						
DFET	30	3	1	1	13	1		1			
DFV0	28	2	•	•	6	•		•			
DJ94	34	3	2	1	12						
HIH	30	3	-	•	10						
DFJT	28	2	3		11						
HLJ	29	2	1	1	11						
37360	29	2	1	1	13	1					
0L7	20	2	•	•	14	•					
0R1	17	1			12						
OR8	25	2			13	1					
0TI	25	2	1		12						
Total	747	72	20	13	318	7	0	1			
Discordance (%)		9.6	2.7	1.7		2.2	0.0	0.3			
Concordance (%	)	90.4	97.3	98.3		97.8	100.0	99.7			

Relationship Animal_ID	Dam r05029	Progeny 1 r17099	Sire r07010	Progeny 2 r17041	Progeny 3 r17061			
Assay	MiSeq DSR SAVAGE	MiSeq DSR SAVAGE	MiSeq DSR SAVAGE	MiSeq DSR SAVAGE	MiSeq DSR SAVAGE	Ambiguous Allele Group		
Mamu-A Major Alleles Mamu-A1*001g2 Mamu-A1*002:01 Mamu-A1*004g1 Mamu-A1*008g1 Mamu-A1*059:01 Mamu-A1*059:01	335 136 1 151 137 1	168 27 1 126 51 1	158 62 1 306 79 1	352 36 1 228 36 1	210 74 1 447 127 1	A1*001:01,A1*001:02 A1*004_6_alleles A1*008_5_alleles A1*023:01,A1*023:02,A1*106:01		
Mamu-A Minor Alleles Mamu-A2*05g1 Mamu-A3*13_A4*14g1 Mamu-A3*13g1 Mamu-A4*14g1 Mamu-E Alleles	77 79 1 145 104 1	319 25 1 164 23 1	712 162 1 93 85 1	423 15 1 97 31 1 199 29 1	438 56 1 91 88 1	A2*05_32_alleles A3*13_7_alleles,A4*14_1_allele A3*13:03,A3*13:11 A4*14_14_alleles		
Mamu-E*02g1 Mamu-E*02g4 Mamu-E*02g5 Mamu-E*02g7 Mamu-E*02g8 Mamu-B Major Alleles	775 185 1 307 106 1 1104 134 1 689 116 1	1923 169 1 1914 92 1	2041 303 1 467 152 1 781 85 1	3240 125 1 634 50 1	914 120 1 382 95 1 1583 69 1 710 85 1	E*02_9_alleles E*02:13,E*02:21,E*02:29 E*02:04,E*02:06 E*02:12:01,E*02:28 E*02:20,E*02:30		
Mamu-B*001g1 Mamu-B*007:07 Mamu-B*007g1 Mamu-B*012:01 Mamu-B_022g1 Mamu-B*027g1			161 60 1 25 161 33 1	143 28 1 27 132 12 1 93 32 1	284 60 1 171 46 1	B*001_alleles B*007_6_alleles B*022:01,B*022:02 B*027:03,B*027:04		
Mamu-B*030g1 Mamu-B*030g2 Mamu-B*031:03 Mamu-B*031g1 Mamu-B*041g1 Mamu-B*043:01	128 47 1	270 12 1 105 12 1 57 24 1 223 18 1	303 73 - 306 79 1 139 26 1	318 11 1 306 29 1 263 16 1	671 103 1 198 35 1 127 40 1 220 41 1	B*030_6_alleles B*030:02,B*030:05 B*031:01,B*031:02 B*041:01,B*041:02		
Mamu-B*048:01 Mamu-B*052:01 Mamu-B*055:01 Mamu-B*058:02 Mamu-B*073:01 Mamu-B*073:g1 Mamu-B*074:g1	275 91 1 54 63 1 180 65 1 177 43 1 179 56 1	318 26 1 44 31 1 129 19 1	140 60 1	- 18 1	149 32 1 16 48 1	B*073:01,B*073:02 B*074:01,B*074:02,B*074:03		
Mamu-B Minor Alleles Mamu-B*035_B*049g1 Mamu-B*053g1 Mamu-B*054:01 Mamu-B*054:04 Mamu-B*054:05 Mamu-B*057:01	161 92 1 194 95 1			293 37 1 321 26 1	261 80 1 114 59 1 169 59 1 104 41 1	B*035:01,B*035:02,B*049:01 B*053:02,B*053:03		
Mamu-B*057:06 Mamu-B*057g1 Mamu-B*063:03 Mamu-B*063:05 Mamu-B*063g1	198 74 1 121 74 1	59 24 1 122 29 1	113 61 1 184 73 1	152 10 1 243 16 1	51 40 1	B*057_alleles  B*063:01_alleles,B*063:02:02_allele		
Mamu-B*070g2 Mamu-B*072g1 Mamu-B*092g1 Mamu-B*098g1 Mamu-B*109:06	28 100 1 198 108 1 479 92 1	218 41 1 - 35 1 479 49 1	447 161 1 14 88 1	365 25 1 23 25 1 324 32 1	89 68 1 330 74 1 82 84 1 238 60 1	B*070:01,B*070:06 B*072_8_alleles B*092:01,B*092:02,B*092:03 B*098_9_alleles		
Mamu-B*134g2 Mamu-B*188g1 Mamu-B11L*01:12 Mamu-B11L*01g1 Mamu-B16*01:01 Mamu-B16*01g1	257 82 1 - 58 1 181 74 1	276 24 1  - 29 -  - 36 1  44 34 1	336 42 1 - 89 1 - 79 1 72 61 1	535 11 1	- 74 1 110 29 1	B*134:03,B*134:04,B*134:06 B*188:01,B*188:02 B11L*01_alleles,B11L*01:04,B11L*01:05 B16*01_alleles		
Mamu-B16*01g2 Mamu-B17*01g1 Mamu-B17*01g2 Mamu-B17*01g4 Mamu-B20*01:02	1305 74 1	773 18 1	51 47 1 593 24 1 6 304 43 1	77 14 - 1221 12 1 971 9 1	1227 17 1	B16*01:02,B16*01:09 B17*01_14_alleles B17*01_9_alleles B17*01:09,B17*01:15		
Mamu-B20*01g1 Mamu-I Alleles Mamu-1*01g1 Mamu-1*01g3	176 66 1 130 63 1	181 21 1 129 31 1	272 82 1 485 151 1	365 33 1 532 44 1 81 28 1	252 68 1	B20*01:01,B20*01:04 I_01_66_alleles I*01:19,I*01:20:01		

Fig. 1 Comparison of MHC class I results from MiSeq PCR amplicon versus whole exome genotyping strategies for a representative breeding group of rhesus macaques

Relationship Animal_ID	Dam r05029 MiSeq DSR SAVAGE					Sire r07010		Progeny 2 r17041		Progeny 3 r17061						
Assay			MiSeq DSR SAVAGE		MiSeq DSR SAVAGE		MiSeq DSR SAVAGE		MiSeq DSR SAVAGE		GE	Ambiguous Allele Group				
Mamu-DRB Alleles																
Mamu-DRB1*03:09	198	370	1	72	131	1	170	305	1	272	107	1	156 20	0 1		
Mamu-DRB1*03g1				2789	217	1	2714	497	1				3052 49	9 1		DRB1*03:06,DRB1*03:26
Mamu-DRB1*10:03				1761	168	1	1952	358	1				2711 31	0 1		
Mamu-DRB*W2g1	154	451	1	72	183	1	132	410	1	206	176	1	107 39	8 1		DRB*W2:01,DRB*W2:05
Mamu-DRB*W3g1	1936	546	1							3097	217	1				DRB*W3:03:01,DRB*W3:03:02
Mamu-DRB*W4:01	1777	414	1							2631	158	1				
Mamu-DQA/DQB Alleles																
Mamu-DQA1*01:02				2384	98	1	2444	256	1				2964 15	4 1		
Mamu-DQA1*01g1	2298	318	1	2046	96	1	2276	288	1	4317	107	1	3360 21	0 1		DQA1*01:04:01,DQA1*01:04:02
Mamu-DQA1*23:01	2883	334	1							5079	108	1				
Mamu-DQB1*06:01	3803	160	1	3980	41	1	3892	152	1	5757	33	1	3892 12	2 1		
Mamu-DQB1*06g2				5229	173	1	4784	345	1				6400 28	2 1		DQB1*06:05,DQB1*06:18
Mamu-DQB1*18g4	2656	329	1							4504	108	1				DQB1*18:02,DQB1*18:27
Mamu-DPA/DPB Alleles																
Mamu-DPA1*02g1	5450	1765	1	5301	316	1	5153	840	1	8727	758	1				DPA1*02_9_alleles
Mamu-DPA1*04g1				435	181	1	489	385	1				1075 35			DPA1*04:03:01,DPA1*04:03:02,DPA1*04:05
Mamu-DPA1*11:01													- 22			
Mamu-DPB1*02g1	106	25	1	87	73	1							342 47	7 1		DPB1*02:01,DPB1*02:04:01,DPB1*02:04:02
Mamu-DPB1*15g1	254	217	1	286	31	1	207	129	1	3084	60	1				DPB1*15:01,DPB1*15:02
Mamu-DPB1*16:01													1769 98	3 1		

Fig. 2 Comparison of MHC class II results from MiSeq PCR amplicon versus whole exome genotyping strategies for a representative breeding group of rhesus macaques



Relationship GS ID	Ave Length	Dam r05029	Progeny 1 r17099	Sire r07010	Progeny 2 r17041	Progeny 3 r17061	Ambiguous Allele Groups
MHC Haplotype 1	Ü	a	a	b	c	b	
MHC Haplotype 2			b			f	
Mamu-DRB Alleles							
Mamu-DRB1*03:09	1,763	3384	761	1053	559	3057	
Mamu-DRB1*03g1	866		1131	768		700	DRB1*03:06,DRB1*03:26
Mamu-DRB1*10:03	653		631	710		618	
Mamu-DRB*W2g1	591	655	520	556	613	612	DRB*W2:01,DRB*W2:05
Mamu-DRB*W3g1	2,213	1430			2996		DRB*W3:03:01,DRB*W3:03:02
Mamu-DRB*W4:01	691				737		
Mamu-DQA/DQB All	eles		_			•	
Mamu-DQA1*01:02	1,942		2087	1475		2264	
Mamu-DQA1*01g1	1,677	1467	1988	1429	1980	1522	DQA1*01:04:01,DQA1*01:04:02
Mamu-DQA1*23:01	2,073				2076		
Mamu-DQB1*06:01	2,820	2726	1334	3199	4063	2780	
Mamu-DQB1*06g2	2,436		1076	3257		2975	DQB1*06:05,DQB1*06:18
Mamu-DQB1*18g4	4,332	4336			4328		DQB1*18:02,DQB1*18:27
Mamu-DPA/DPB Alle	les		_			•	
Mamu-DPA1*02g1	1,897	1989	1795	1929	1873		DPA1*02_9_alleles
Mamu-DPA1*04g1	1,985		1894	2051		2011	DPA1*04:03:01,DPA1*04:03:02,DPA1*04:05
Mamu-DPA1*11:01	1,842				_	1842	
Mamu-DPB1*02g1	3,693		3946	3073		4059	DPB1*02:01,DPB1*02:04:01,DPB1*02:04:02
Mamu-DPB1*15g1	2,687	2470	2506	3190	2581		DPB1*15:01,DPB1*15:02
Mamu-DPB1*16:01	827					827	

MHC Haplotype		b				f
Mamu-A Haplotype	A004	A001	A008	A002a	A023	A002a
Mamu-B Haplotype	B048	В043ь	B001a	B055	B043a	B012b
Mamu-DRB Haplotype	DR04a	DR03f	DR04a		DR06	DR04a
Mamu-DQA	01g1	01:02	01g1	23:01	23:01	01g1
Mamu-DQB	06:01	06g2	06:01	18g4	18g4	06:01
Mamu-DPA	02g1	04g	02g1	02g1	02g1	11:01
Mamu-DPB	15g	02g	15g	15g	15g	16:01

**Fig. 3** Lengths of MHC sequence contigs assembled by the SAVAGE method for a representative breeding group of rhesus macaques. Values in the body of this figure indicate contig lengths generated for these MHC sequences in each animal.

- (A) MHC class I genotyping results are illustrated for the five animals in this breeding group. Three false negative allele calls for SAVAGE versus the expected genotypes for these animals are highlighted in magenta, e.g., Mamu-B\*030g1 in sire r07010. Sequences highlighted in red are associated with the maternal MHC Haplotype a that was inherited by Progeny 1 from its dam. Sequences in Progeny 1 and Progeny 3 for their MHC Haplotype b that was inherited from sire r07010 are highlighted in dark blue while the light blue sequences represent the alternate paternal Haplotype c that was inherited by Progeny 2. Three unique extended Haplotypes in this breeding group are indicated with shades of grey (d-f). MHC allele groups that are shared by both parental haplotypes are indicated by colored borders around filled cells.
- (B) MHC class II genotyping results are illustrated for this same breeding group.
- (C) Abbreviated Mamu haplotype designations are summarized for the sx extended MHC haplotypes identified by segregation in this breeding group. For example, the twenty MHC sequences (red) that are associated with extended Haplotype a can be summarized by the following string of abbreviated Mamu haplotype designations: Mamu-A004/B048/DR04a/DQA01g1/DQB06:01/DPA02g1/DPB15g (Karl et al 2013).

# Supplementary Table 1. Fraction of exome sequence reads corresponding to MHC class I and class II genes after target capture with the VCRome 2.1 probe design alone

		MHC-I	DRB1/3/4/5	DQA1	DQB1	DPA1	DPB1	MHC	
	Total Raw	Reads	Reads	Reads	Reads	Reads	Reads	Reads	MHC %
GS ID SRA Accession	Reads	Extracted	Extracted	Extracted	Extracted	Extracted	Extracted	Extracted	of total
cy0642 SAMN11281734	79,795,404	4,848	26,822	2,568	2,274	900	81,340	118,752	0.15
cy0643 SAMN11281735	86,265,844	4,408	26,930	2,542	2,320	936	74,370	111,506	0.13
cy0646 SAMN11281736	109,909,444	4,724	25,476	2,382	2,196	910	72,206	107,894	0.1
cy0648 SAMN11281737	106,315,304	5,558	34,442	2,966	2,714	1,092	97,254	144,026	0.14
cy0649 SAMN11281738	78,575,038	6,022	33,742	3,176	2,970	1,134	90,556	137,600	0.18
cy0651 SAMN11281739	102,890,862	6,686	33,194	3,388	3,094	1,294	94,532	142,188	0.14
cy0652 SAMN11281740	89,074,544	4,652	25,314	2,660	2,478	976	69,976	106,056	0.12
cy0654 SAMN11281741	99,169,798	5,294	30,328	2,924	2,756	1,042	79,664	122,008	0.12
Average	93,999,530	5,274	29,531	2,826	2,600	1,036	82,487	123,754	0.13